

Gravitational Waves from Collapsing Vacuum Domains

Marcelo Gleiser* and Ronald Roberts†

Department of Physics and Astronomy, Dartmouth College, Hanover, NH 03755, USA
(DART-HEP-98/03 October 9, 2018)

The breaking of an approximate discrete symmetry, the final stages of a first order phase transition, or a post-inflationary biased probability distribution for scalar fields are possible cosmological scenarios characterized by the presence of unstable domain wall networks. Combining analytical and numerical techniques, we show that the non-spherical collapse of these domains can be a powerful source of gravitational waves. We compute their contribution to the stochastic background of gravitational radiation and explore their observability by present and future gravitational wave detectors.

04.30.Db, 98.80.Cq

In order to further our understanding of the physical processes that took place early in the history of the Universe we should explore potential events which may have left an imprint detectable by current or future experiments. One exciting possibility is that certain primordial processes generated a stochastic background of gravitational waves. During the past decade or so, several cosmological sources (as distinguished from astrophysical sources such as coalescing binary systems [1]) of stochastic gravitational waves have been proposed [2]. These include inflationary models [3], cosmic strings [4], strong first order phase transitions [5,6], and nontopological solitons [7].

All ground-based detectors (interferometric or resonant bar), such as LIGO or VIRGO, probe the frequency interval $10\text{Hz} \lesssim f \lesssim 10^4\text{Hz}$. Lower frequencies are to be probed in space, as with the planned LISA mission, which has a projected sensitivity of $10^{-4}\text{Hz} \lesssim f \lesssim 1\text{Hz}$.

Here we propose another powerful source of primordial gravitational waves, the non-spherical collapse of bounded domain walls, or bags, which separate different vacuum regions. Zel'dovich *et al.*, have shown that the appearance of domain walls is a direct consequence of the breaking of a discrete symmetry [8]. In the same work, domain walls were shown to be incompatible with big-bang cosmology, as they would create a power law expansion ruled-out by observations. Thus, if domain walls were created they had to disappear. One of the mechanisms proposed by Zel'dovich *et al.* was to consider an *approximate* discrete symmetry as opposed to an exact one; the difference in energy density between the two vacua generates a pressure force that eliminates the walls. Other scenarios for the disappearance of the domain walls were investigated in Ref. [9].

The existence of walls and other topologically stable

defects were explored by Kibble, who also suggested the possibility of an approximate symmetry as a mechanism to eliminate the walls [10]. Several authors explored this idea further [11,9]. Recently, it was shown that unstable domain walls could also be created during a post-inflationary non-thermal phase transition [12]. The evolution of the unstable domain-wall network has been studied numerically [13] and analytically [14].

We can envisage at least three scenarios where unstable domain wall networks can be generated: i) the breaking of an approximate discrete symmetry in a thermal phase transition; ii) biased fluctuations in a non-thermal post-inflationary scenario; iii) during the final stages of a first order phase transition, as bubbles of the true vacuum percolate, leaving a disconnected network of shrinking false vacuum domains.

We can model all these scenarios with a biased double-well potential for a real scalar field,

$$V(\phi) = \frac{\lambda}{4} (\phi^2 - \phi_0^2)^2 + h\phi_0\phi \left(\frac{1}{3}\phi^2 - \phi_0^2 \right), \quad (1)$$

where $h > 0$ is a dimensionless constant which biases the potential towards the $+\phi_0$ minimum. The energy density difference between the two minima is $\Lambda = \frac{4}{3}h\phi_0^4$, while the energy density barrier between the maximum at $\phi_0 = -(h/\lambda)\phi_0$ and the global minimum ($+\phi_0$) is $B = \frac{\lambda}{4}\phi_0^4[1 - \mathcal{O}(h/\lambda)]$. Coordinates scale as $\tilde{x} = \sqrt{\lambda}\phi_0 x$, while energies scale as $\tilde{E} = (\sqrt{\lambda}/\phi_0) E$.

The formation of a domain wall network during a phase transition has been discussed in several works [10,4,9,12]. There are two possibilities, determined by the probability the field has of landing on either vacuum, p_{\pm} . There is a critical “percolation probability” for a given vacuum, p_c . For cubic lattices, $p_c = 0.31$, the value we will adopt here [15]. If both p_+ and p_- are larger than p_c both vacua percolate, being separated by a domain wall stretching across the lattice. At formation, the wall will be rather convoluted, with local average curvature given by the typical fluctuation scale, the correlation length ξ . If only $p_+ > p_c$, most of the volume will be in the $+$ -vacuum, with isolated clusters (bags) of the negative vacuum with a distribution function, $f(r) \sim r^{-1.5} \exp[-r]$, where r is the number of cells of unit volume $V_{\xi} \simeq \xi^3$ in a given cluster [15]. We will call this case the “no-percolation” case.

The energy density of an isolated domain is given by

$$\rho[\phi_b] = \frac{1}{2} \left(\frac{\partial \phi_b}{\partial t} \right)^2 + \frac{1}{2} \nabla \phi_b \cdot \nabla \phi_b + V(\phi_b), \quad (2)$$

where $\phi_b(\mathbf{x}, t)$ is the field configuration describing the bag at time t . We define the average radius of an isolated domain by $R_{\text{av}} = (\int dV |\mathbf{x}| \rho[\phi_b]) / \int dV \rho[\phi_b]$.

Two forces will act on the walls; the tension, P_T , which will act to straighten the walls, and the vacuum pressure, P_Λ , which will cause the domains to shrink. Here, we will consider two possibilities. First, the “no-percolation case”, where the false vacuum bags disappear very quickly after they form, that is, with $P_\Lambda > P_T$ right at formation. This case is characterized by having several small bags within the horizon. Second, we will consider the “percolation case”, where the tension force will straighten the walls for a while, up to the horizon scale, before the vacuum pressure acts to accelerate the walls against each other, causing the formation of large unstable bags [9].

We compute the output in gravitational radiation from the collapsing domains within the full, linearized gravity approximation [16]. More details will be provided in a forthcoming publication. In the meantime, the reader may consult Ref. [6], as we follow a similar approach.

The computation of the spectrum in gravitational waves from collapsing 3-dimensional domains in the linearized gravity approximation is a rather cumbersome and computer-intensive task. As the authors of Ref. [6], we have limited ourselves here to studying the spectrum for situations with axial symmetry. In our case, as toy models to more realistic bag configurations, we considered two types of domains, ellipsoids and deformed Gaussians. Contrasting our results with the full 3-dimensional calculations for the simpler quadrupole approximation, we conclude that here we are providing a lower bound for the total output in gravitational radiation.

The total energy radiated in the direction $\hat{\mathbf{k}}$ into the solid angle Ω at frequency ω is given by,

$$\frac{dE_{\text{GW}}}{d\omega d\Omega} = G\omega^2 [T^{zz}(\hat{\mathbf{k}}, \omega) \sin^2 \theta + T^{xx}(\hat{\mathbf{k}}, \omega) \cos^2 \theta - T^{yy}(\hat{\mathbf{k}}, \omega) - 2T^{xz}(\hat{\mathbf{k}}, \omega) \sin \theta \cos \theta]^2 \quad (3)$$

where $T^{ij}(\hat{\mathbf{k}}, \omega)$ are the Fourier-transformed spatial components of the energy momentum tensor for the field configuration ϕ_b [6].

From simple scaling arguments, the integrated energy radiated in gravitational waves can be written as,

$$E_{\text{GW}}(R_{\text{av}}) = \epsilon(R_{\text{av}}) G \sigma^2 R_{\text{av}}^3, \quad (4)$$

where σ is the surface energy density for the domains, and $\epsilon(R_{\text{av}}) \equiv \epsilon_0 \left(\frac{R_{\text{av}}}{\xi_0}\right)^\alpha$ is the efficiency parameter, with ϵ_0 a number to be determined. ξ_0 is the $T = 0$ correlation length.

For ellipsoids, we wrote

$$\phi_b(r, z) = \phi_+ + \frac{(\phi_- - \phi_+)}{2} \left(1 - \tanh(\varepsilon/\sqrt{2})\right), \quad (5)$$

where ε is the solution of $r^2/(a + \varepsilon)^2 + z^2/(b + \varepsilon)^2 = 1$. For deformed Gaussians, we wrote,

$$\phi_b(r, \theta) = \phi_+ + (\phi_- - \phi_+) \exp \left[-\frac{r^2}{[R_0(1 + \delta R)]^2} \right], \quad (6)$$

where $\delta R = \sum_{l,m} R_{l,m} Y_{l,m}(\theta, \varphi)$ measures the distortion from spherical symmetry. For axial symmetry we kept $m = 0$. These configurations are then used as initial data for solving numerically the Klein-Gordon equation for $\phi(r, z, t)$. As the configuration evolves in time, we compute the emission of gravitational radiation using Eq. 3.

As shown in Fig. 1, the energy of the initial configurations can be well fitted by $E_0(R_{\text{av}}) = E_0^0 \left(\frac{R_{\text{av}}}{\xi_0}\right)^\gamma$. For spherically symmetric domains with degenerate vacua $\gamma = 2$. Writing also $E_0(R_{\text{av}}) = \sigma R_{\text{av}}^2$, we obtain that the surface tension scales as $\sigma = \frac{E_0^0}{\xi_0^2} \left(\frac{R_{\text{av}}}{\xi_0}\right)^{\gamma-2}$. From left to right, the sample points shown are: for ellipsoids $(a, b) = [(3, 1.5), (2, 4), (4, 2), (4, 6), (6, 4), (6, 10), (10, 6)]$; for deformed Gaussians $(\ell, R_0, \delta R) = [(4, 3.5), (3, 3.5), (4, 4.8), (3, 5.3), (4, 5.5), (4, 6.8), (4, 8.5)]$.

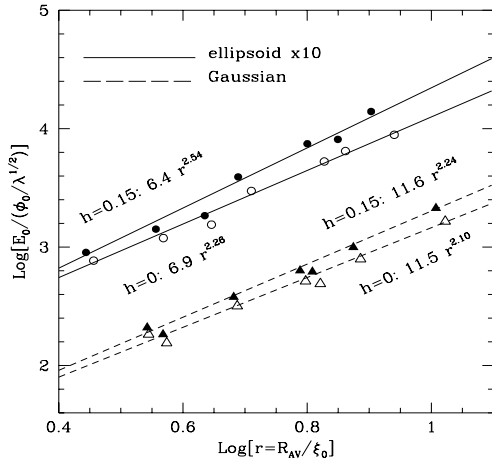


FIG. 1. The initial energy of the nonspherical domains vs. their average radius for degenerate ($h = 0$) and nondegenerate ($h = 0.15$) potentials. The power law fits are shown explicitly.

In Fig. 2, we show the integrated energy in gravitational waves, which can be fitted by a simple power law relation, $[M_{Pl} = 1.2 \times 10^{19} \text{ GeV}$ is the Planck mass]

$$E_{\text{GW}}(R_{\text{av}}) = E_{\text{GW}}^0 \left(\frac{\phi_0}{M_{Pl}}\right)^2 \left(\frac{R_{\text{av}}}{\xi_0}\right)^\beta. \quad (7)$$

Comparing Eqs. 4 and 7, we obtain that $\beta = \alpha + 2\gamma - 1$, and $\epsilon_0 = \frac{E_{\text{GW}}^0}{\sqrt{2}(E_0^0)^2} [2\sqrt{\lambda}]^{-1}$. The quantities with a tilde are dimensionless quantities and the quantity in the squared brackets comes from including thermal corrections to the correlation length, $\xi(T_G) = \xi_0 / (2\sqrt{\lambda}) = \frac{1}{\sqrt{2}\lambda T_G}$, evaluated at the Ginzburg temperature $T_G^2 \simeq 4\phi_0^2 / (1 + 4\lambda)$,

the temperature where the wall network forms in a thermal phase transition [10,9].

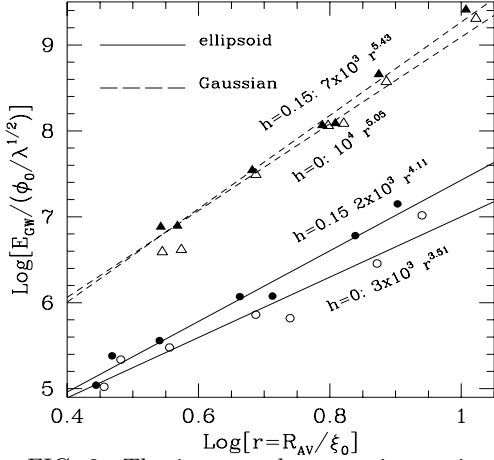


FIG. 2. The integrated output in gravitational radiation generated during the collapse of the nonspherical domains vs. their initial average radius. The sample points shown are the same as in Fig. 1.

Since the time-scale of collapse is well approximated by the average size of the domains, the rate of emission is,

$$\dot{E}_{\text{GW}} \simeq \sqrt{2} \tilde{E}_{\text{GW}}^0 [2\sqrt{\lambda}] \left(\frac{\phi_0^4}{M_{\text{Pl}}^2} \right) \left(\frac{R_{\text{av}}}{\xi_0} \right)^{\beta-1}. \quad (8)$$

The energy density in gravitational radiation for clusters with r and $r + dr$ cells in a time interval between t and $t + dt$ is

$$d\rho_{\text{GW}} \simeq \dot{E}_{\text{GW}} n(r) dr dt, \quad (9)$$

where $r \simeq (R_{\text{av}}/\xi)^3$, and the number density of r -clusters can be written as $n(r) = Cr^{-1.5}e^{-r}/V_\xi$. Demanding that the bags occupy a fraction p_- of the horizon volume ($p_- < p_c$), we can fix the normalization constant as $C \simeq e p_-$.

The typical bag lifetime τ is of order $R_{\text{av}} \ll \lambda_H$, where $\lambda_H = (45/4\pi^3 g_*)^{1/2} M_{\text{Pl}}/T^2$ is the horizon length and g_* is the number of relativistic degrees of freedom at temperature T . The total output in gravitational radiation is thus,

$$\rho_{\text{GW}} \simeq 2\sqrt{2} C \lambda [2\sqrt{\lambda}]^3 \tilde{E}_{\text{GW}}^0 \phi_0^4 \left(\frac{\phi_0}{M_{\text{Pl}}} \right)^2 f_\beta(r_{\text{max}}), \quad (10)$$

where $f_\beta(r_{\text{max}}) \equiv \int_1^{r_{\text{max}}} r^{\beta/3-3/2} e^{-r} dr$, is $\mathcal{O}(1)$ for all interesting values of its parameters.

Using that the Universe is radiation-dominated with energy density $\rho_{\text{rad}} = (\pi^2/30) g_* T^4$, the fraction in energy density from gravitational waves is, neglecting factors of $\mathcal{O}(1)$, and using $T_G \simeq 2\phi_0$,

$$\Omega_{\text{GW}} \simeq 10^2 \lambda [2\sqrt{\lambda}]^3 \left(\frac{\tilde{E}_{\text{GW}}^0}{10^4} \right) \left(\frac{100}{g_*} \right) \left(\frac{\phi_0}{M_{\text{Pl}}} \right)^2. \quad (11)$$

Since the domains will mostly have linear dimensions of order $R_{\text{av}} \sim \xi$, the dominant frequency of emission is $\omega \simeq 1/R_{\text{av}} \simeq \sqrt{2\lambda} [2\sqrt{\lambda}] \phi_0$. Redshifting these quantities we obtain,

$$h^2 \Omega_{\text{GW}}^0 \simeq \frac{1.7 \times 10^{-3}}{[2\sqrt{\lambda}]^{-3}} \left(\frac{100}{g_*} \right)^{\frac{3}{2}} \left(\frac{\tilde{E}_{\text{GW}}^0}{10^4} \right) \lambda \left(\frac{\phi_0}{M_{\text{Pl}}} \right)^2, \quad (12)$$

and, $f^0 \simeq 1.3 \times 10^{10} \sqrt{\lambda} [2\sqrt{\lambda}] \left(\frac{100}{g_*} \right)^{\frac{1}{3}} \text{ Hz}$.

Using that the detector strain at wave band given by observational frequency f for stochastic gravitational radiation is $h_c(f) \equiv 1.3 \times 10^{-18} [h^2 \Omega_{\text{GW}}^0]^{1/2} (\text{Hz}/f)$ [17], we get

$$h_c(f) \simeq \frac{4.1 \times 10^{-30}}{[2\sqrt{\lambda}]^{-1/2}} \left(\frac{\tilde{E}_{\text{GW}}^0}{10^4} \right)^{\frac{1}{2}} \left(\frac{100}{g_*} \right)^{\frac{5}{12}} \left(\frac{\phi_0}{M_{\text{Pl}}} \right). \quad (13)$$

The no-percolation case is characterized by a very high frequency spectrum and small amplitudes, beyond the presently projected sensitivity of ground-based interferometers. The situation is quite different for the percolating case.

When both vacua percolate, they are separated by a convoluted domain wall, with initial average curvature $R_{\text{av}} \simeq \xi$. The tension force dominates the wall dynamics for a while, until the vacuum pressure starts accelerating the walls against each other, eventually causing the formation of large, unstable domains. In order for this to happen, the asymmetry must satisfy $h < \frac{3\sqrt{2}}{2} \lambda [2\sqrt{\lambda}]^3 \tilde{E}_{\text{GW}}^0$, while, for the walls to disappear as their average curvature reaches cosmologically significant scales ($R_{\text{av}} \lesssim \lambda_H$), $h \gtrsim (\lambda)^{1/2+(\gamma-2)} (\sqrt{g_*} \phi_0 / M_{\text{Pl}})^{3-\gamma} \tilde{E}_{\text{GW}}^0$. To these bounds we add the percolation constraint, $p_- \geq 0.31$, which becomes, $h \leq 0.15 \lambda$ [9].

Writing the average radius of the domains as $R_{\text{av}} \equiv a \lambda_H$, the energy density in gravitational waves from collapsing domains is, (a is not the same as the ellipsoidal axis) $\rho_{\text{GW}} \simeq \frac{\dot{E}_{\text{GW}}}{a^2 \lambda_H^2}$, or with $\kappa \equiv 45/32\pi^3$,

$$\rho_{\text{GW}} \simeq \frac{2 \tilde{E}_{\text{GW}}^0 \phi_0^4 a^{\beta-3} \lambda^{(\beta-1)/2}}{\kappa^{(3-\beta)/2} g_*^{(\beta-3)/2}} \left(\frac{\phi_0}{M_{\text{Pl}}} \right)^{5-\beta}. \quad (14)$$

The typical frequency will be, $f_{\text{av}} \simeq [2\pi a \lambda_H]^{-1}$, which redshifts to

$$f^0 \simeq 6.1 \times 10^{11} a^{-1} \left(\frac{g_*}{100} \right)^{\frac{1}{6}} \left(\frac{\phi_0}{M_{\text{Pl}}} \right) \text{ Hz}, \quad (15)$$

while the fraction of the energy density in gravitational waves today is

$$h^2 \Omega_{\text{GW}}^0 \simeq \frac{6.7 \times 10^{-\beta+1} \left(\frac{\tilde{E}_{\text{GW}}^0}{10^4} \right) \left(\frac{100}{g_*} \right)^{\frac{\beta-1}{2}}}{a^{3-\beta} \lambda^{(1-\beta)/2} \kappa^{-\beta/2}} \left(\frac{\phi_0}{M_{\text{Pl}}} \right)^{5-\beta}. \quad (16)$$

The detector strain in the wave band f is given by,

$$h_c(f) \simeq \frac{1.7 \times 10^{-29-\frac{\beta}{2}} \left(\frac{\tilde{E}_{\text{GW}}^0}{10^4} \right)^{\frac{1}{2}} \left(\frac{100}{g_*} \right)^{\frac{\beta+1}{4}}}{a^{(1-\beta)/2} \lambda^{(1-\beta)/4} \kappa^{-\beta/4}} \left(\frac{\phi_0}{M_{\text{Pl}}} \right)^{\frac{3-\beta}{2}}. \quad (17)$$

We have summarized our results in Fig. 3, where the detector strain vs. frequency are plotted for several values of β and compared with the LIGO (initial and advanced) and LISA sensitivities. The solid squares locate an electroweak phase transition at $T = 200$ GeV. The solid triangles, a hypothetical transition at $T = 10^9$ GeV. Continuous curves are for ellipsoids while dashed curves are for Gaussians. The dot-dashed curve is for a Gaussian with $a = 10^{-2}$. LIGO is mostly sensitive to collapsing walls at $\phi_0 \sim 10^9$ GeV or so, while LISA can probe the electroweak phase transition for a comfortable range of parameters. The spectrum from collapsing bags, being very pronounced at a given frequency, is quite different from the mostly flat spectra of cosmic strings and inflationary models [2]. A more detailed analysis will be presented in a forthcoming publication.

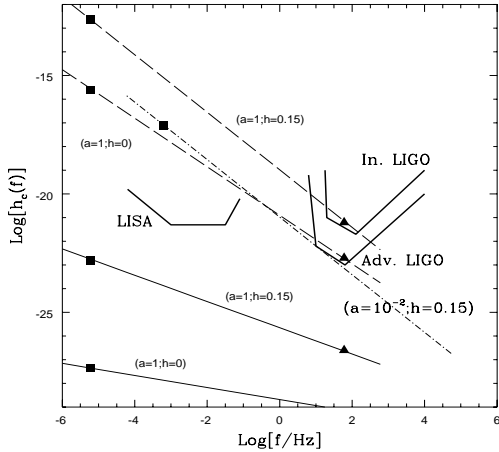


FIG. 3. Predicted detector strain vs. dominant frequency band from collapsing nonspherical domains. We also display the sensitivities of the LIGO and LISA detectors. The solid cubes are for an electroweak transition at $T = 200$ GeV and the solid triangle for a hypothetical transition at $\phi_0 = 10^9$ GeV.

It is clear that the stochastic background of gravitational waves left behind from collapsing domain walls can be detectable for several situations of interest, illustrating the potential impact of gravitational wave astronomy on applications of particle physics to the early Universe.

The authors were partially supported by the NSF through a Presidential Faculty Fellows Award no. PHY-9453431 and by a NASA grant no. NAG5-6613.

- [1] É. É. Flanagan, *Astrophysical Sources of Gravitational Radiation and Prospects for Their Detection*, to appear in Proceedings of GR15, Pune, India, 1997 [gr-qc/9804024].
- [2] B. Allen, in *Les Houches School on Astrophysical Sources of Gravitational Waves*, eds. J. A. Marck and J. P. Lasota (Cambridge University Press, Cambridge, England, 1996) [gr-qc/9604033].
- [3] M. S. Turner, Phys. Rev. D **55** (1997) 435; B. Allen and R. Brustein, Phys. Rev. D **55** (1997) 3260; C. Baccigalupi, L. Amendola, P. Fortini, and F. Occhionero, Phys. Rev. D **54** (1997) 4610, and references therein.
- [4] A. Vilenkin, Phys. Rep. **121** (1985) 263; R. R. Caldwell and B. Allen, Phys. Rev. D **45** (1992) 3447; X. Martin and A. Vilenkin, Phys. Rev. Lett. **77** (1996) 2879.
- [5] M. S. Turner and F. Wilczek, Phys. Rev. Lett. **65** (1990) 3080; C. J. Hogan, Mon. Not. R. Astron. Soc. **218** (1986) 629; E. Witten, Phys. Rev. D **30** (1984) 272.
- [6] A. Kosowsky, M. Turner, and R. Watkins, Phys. Rev. D **45** (1992) 4514; M. Kamionkowski, A. Kosowsky, and M. Turner, Phys. Rev. D **49** (1994) 2837.
- [7] M. Gleiser, Phys. Rev. Lett. **63** (1989) 1199.
- [8] Ya. B. Zel'dovich, I. Yu. Kobzarev, and L. B. Okun, Zh. Eksp. Teor. Fiz. **67** (1974) 3 [Sov. Phys. JETP **40** (1975) 1].
- [9] G. Gelmini, M. Gleiser, and E. W. Kolb, Phys. Rev. D **39** (1989) 1558.
- [10] T. W. B. Kibble, J. Phys. A **9** (1976) 1387.
- [11] A. Vilenkin, Phys. Rev. D **23** (1981) 852; P. Sikivie, Phys. Rev. Lett. **48** (1982) 1156; F. W. Stecker, Phys. Lett. B **143** (1984) 351.
- [12] Z. Lalak, S. Thomas, and B. A. Ovrut, Phys. Lett. B **306** (1993) 10; Z. Lalak, S. Lola, B. Ovrut, and G. G. Ross, Nucl. Phys. B **434** (1995) 675.
- [13] D. Coulson, Z. Lalak, and B. Ovrut, Phys. Rev. D **53** (1996) 4237; S. E. Larrson, S. Sarkar, and P. L. White, Phys. Rev. D **55** (1997) 5129.
- [14] M. Hindmarsh, Phys. Rev. Lett. **77** (1996) 4495.
- [15] D. Stauffer, Phys. Rep. **54** (1979) 1.
- [16] S. Weinberg, *Gravitation and Cosmology* (Wiley, New York, 1972), Ch. 10.
- [17] K. S. Thorne, in *300 Years of Gravitation*, ed. by S. Hawking and B. Israel (Cambridge University Press, Cambridge, England, 1987).